The 11th TSAE International Conference
26-27 April 2018
Available online at www.tsae.asia

Feasibiltiy Study of Evaluation Brix of Sugarcane Using Multispectral Camera Mounted on Unmanned Aerial Vehicle

Chanreaksa Chea[1], Khwantri Saengprachathanarug[1]*, Mahisorn Wongphati[2], Jetsada Posom[1], Cheerawat Nodthaisong[1], Eizo Taira[3]

[1]Faculty of Engineering, Khon Kaen University, Muang, Khon Kaen, 40002, Thailand.
[2]HG Robotics Company Limited, Bangkok Noi, Bangkok, 10700, Thailand
[3]Faculty of Agriculture, University of the Ryukyus, Okinawa 903-0213, Japan
*Corresponding author: Tel: +66-8-7668-9270, E-mail: khwantri@kku.ac.th

Abstract

The possibility application of multispectral imagery using Unmanned Aerail Vehicle (UAV) as platform to predict Brix value in sugarcane field was evaluated. Total 4 flight missions were conducted in November 2017 using rotate-wing UAV and a 5-band MicaSen-RedEdge camera sensor to fly in the afternoon time (around 2:00pm) over an experiment trail which consists of 4 varieties (KK3, K88-92, UT84-12, KK06-501). The sugarcane is new planted, in its 10-month-old with the range of brix 15-21 ^{0}Brix, and grown under rain-fed. After each flight, Brix measurement was done using refractometer with 2 random juice samples in each plot, total 32 samples in this study. Acquired Images were processed in Pix4D mapper software to create reflectance map of each band (Blue, Greem, Red, NIR, and RedEdge). Matlab was used to compute vegetation indices (RVI, NDVI, GNDVI, $SRPI_b$, CI_{green}, and $CI_{rededge}$). Then the calibration equations are determined using simple regression between each vegetation indices and brix value. The result showed that GNDVI has the best correlation with Brix value, Standard Erro (SE) 0.45 ^{0}Brix and R^2 0.86, while the rest vegetation indices have higher SE 0.51-1.13 ^{0}Brix. From preliminary result, it is possible to predict Brix value in the field from spectra of multispectral camera mounted on UAV. The accuracy of model can be improved by adding more data from various concerning environment conditions such as light and temperature, and more range of brix data because datas used in this study are still in early harvest season.

Keywords: Brix, Multispectral, UAV

1 Introduction

Fair payment is a desire of both buyer and grower, which is the main reason to create payment system, for instant, the revolution of sugarcane payment. Heretofore, sugarcane yield was only measured by weight, but due to different end-product purposes, for example sugar product, new dealing methods have developed which new sugarcane payment formula (Figure 1) has depended on sugar content of cane or Commercial Cane Sugar (CCS) which derived from Brix, Pol and Fiber value. Before now, Brix value could be obtained with refractometer machine in laboratory only, but because of the need of real-time result, availability, and flexibility, the hand-held refractometer was invented to facilitate acquiring the accurate result quickly and easy carrying. However, it is still a time-consuming method because we must withdraw fresh juice from sugarcane stalk, so labor is required, and stalks are wounded or sometimes might be broken. Recent researches have introduced using of Near Infrared Spectroscopy (NIR) that has capacity to measure Brix value without destructing stalk. The equipment uses spectrum wavelength to detect Brix value by direct scanning on skin of sugarcane stalks (Mat, 2013) & (Mat, 2014). The study results showed that calibration models made from correlation brix value and detected spectra are accurate. Yet, the prediction brix value of whole field is preferred, so NIR spectroscopy cannot give result in short time as require because it must measure one by one stalk, not the whole field at once time. Meanwhile the breeding programs that do experiments in large fields and need to observe every testing variety in the fields won't prefer to determine needed value from stalk to stalk but they would rather operate measurement methods that are temporal flexibility, fast and precise.

Remote sensing is a part of Precision Agriculture (PA), which has been getting known more and more through a lot of recent studies, especially Unmanned Aerial Vehicles (UAVs) due to its availability, flexibility and high-resolution imagery. The UAVs are adaptability in flight planning and can conduct multiple missions repeatedly which is a great advantage to work with large area easily (Flynn, 2014). In addition, it is accessible to difficult area, or

dangerous zone like flooding area, forest, and river, to collect data since it is enabling to employ by auto-pilot program. Finally, UAVs can obtain very high-resolution imagery of 1- 20 cm which are suitable resolution for site- specific crop management (Wojtowicz, 2015).

However, UAVs still have limited payload, so light multispectral cameras (MCs) are very compatible with UAVs. With multi- spectrum from MCs, numerous vegetation indices (VIs) were created to estimate and describe characteristics of plants at different growth stages. Specific VIs has its unique composition of wavebands that can be linked to specific crop parameters and part of the growing season (Hatfield, 2010).

Several current researches have been conducted to develop new calibration models or methods using UAVs platform equipped with multispectral cameras to study and to estimate numerous parameters of plants and to map those interesting factors for facilitating the use of alternative strategies. A study used UAV for remote sensing to discover and map the nuisance green algae in river for preserve freshwater benthic environments, or prevent replacement of desired species, and the result showed that this lightweight aerial imaging system can provide spatially precise (±0. 3 m horizontal position) and high-resolution (0.25 m) (Flynn, 2014). Similar study also used multispectral remote sensing from unmanned aircraft to map rangeland and found that multispectral imagery acquired from UAV produces high quality of resolution information for rangeland applications with overall accuracy of the image mosaic 87% (Laliberte, 2011) . There are more various applications that multispectral imaging sensors mounted on UAVs can be used to monitor by making relations between vegetation indices and interesting crop parameters, for instance, assessment and mapping vineyard water status variability which calibrated model made from regression between vegetation indices and water status parameter (leaf stomatal conductance and stem water potential) for detecting and solving water stress or drought problem on time (Baluja, 2012) , vegetation monitoring by using Photochemical reflectance index (PRI) and canopy temperature to estimate leaf area index, chlorophyll content (C_{ab}), and water stress detection (Berni, 2009).

The main objective of this study was to demonstrate the possibility of using images gotten from multispectral sensor on UAV platform to calibrate models for estimating Brix value non-destructively and quickly in large area.

Figure 1. Cane Price formula of MSF Sugar Mill (www.msfsugar.com.au)

2 Materials and Methods

2.1 Study Area

The sugarcane field used in this study is located in experimental field of Agriculture Faculty, Khon Kaen University, Thailand. There are 4 varieties, KK3, K88-92, UT84-12, and KK06-501, were chosen to study because some of their specific characteristics such as yield, height and leave formation might have significant effects on study result. There were 4 plots and dimension of each plot is 6mx8m, corresponding to 4 rows per plot. The sugarcanes were grown under rain-fed and nitrogen input 312.5kg/ha, which was applied twice by first time when sugarcane is 3-month-old and second time when it is 6-month-old after the previous harvest. The experiment started in November when the sugarcane was 10-month-old and we conducted experiment once a week, in the afternoon at 1:00 pm. The experiment finished at the end of November, so there are 4 flight missions in total.

2.2 UAV description

A six-rotor VESPA HEX 650 (HG Robotic company, Thailand) (Figure 2, Table 1) was used in this study. It has takeoff weight 4.5kg and a communication distance less than 1200m (2.4GHz). This Unmanned aerial system is equipped with an open-source autopilot hardware based on Pixhawk design (3D Robotics, Inc. USA). Plus, a Global Positioning System (GPS) Mini Ublox NEO-M8N is attached vertically on the UAV, GPS horizontal accuracy is about 2.5 m in good condition, 0.5-0.6 m accuracy of the UAV is from a combination of GPS and other inertia measurement unit (IMU) information, and built-in compass. This aircraft can operate about 10-15 minutes per battery pack, Lipo battery, 10000mAh, 22.2V.

Figure 2. The ready-to-fly six-rotor VESPA HEX 650

Table 1. Summary of UAV specification

Name	VESPA HEX 650
Number of rotors	6
Takeoff weight	4.5kg
Communication distance	1200m
Autopilot system	open-source autopilot hardware
GPS	Mini Ublox NEO-M8N
Operation capacity	10-15 minutes
Battery	Lipo battery, 10000mAh, 22.2V

2.3 *Image Sensor*

A MicaSense-Rededge camera (MicaSense, RedEdge, USA) (Figure 3) was used as the multispectral sensor, its weight is just 150g recommended as suitable loading on a UAV. The specifications of this sensor are listed in table below (Table 2&3).

Figure 3. RedEdge Camera

Table 2. Specifications of Rededge camera.

Dimension	12.1 cm × 6.6 cm × 4.6 cm
External Power	5.0 V DC, 4 W nominal
Spectral Bands	Blue, green, red, red edge, near IR (narrowband)
Ground Sample Distance	8 cm per pixel (per band) at 120 m
Capture Rate	1 capture per second (all bands)
Interface	Serial, Ethernet, GPS
Field of View	47.2° HFOV

(https://www.micasense.com/rededge-m/)

Table 3. Center wavelength and Band width of each band in RedEdge

Band Number	Band Name	Center Wavelength(nm)	Bandwidth FWHM (nm)
1	Blue	475	20
2	Green	560	20
3	Red	668	10
4	Near IR	840	40
5	Red Edge	717	10

(https://support.micasense.com/hc/en-us/articles/225950667-RedEdge-Manual-Specifications)

As mentioned above, MicaSense-RedEdge camera has fast capture rate enables faster flight speeds and lower flight altitudes. The RedEdge camera stores file with format of 16-Bit TIFF, resolution 1280×960 pixels, in the SD card in a folder structure and a new folder will be created for each time the camera is power up.

2.4 *Data Acquisition Missions*

a) *Ground Control Points*

Ground Control Points (GCPs) are characteristic features or objects that have been placed on the scene, and which its GPS coordinate have been measured and recorded. GCPs will help to reduce error accumulation of images during image processing. In this study, we used 6 GCPs which 4 GCPs were placed on each corner of field and the last 2 GCPs are set down in the middle line of both sides of field. The GCPs panel is black-white panel which has dimension 50cm×50cm and each black and white part are 25cm×25cm (Figure 4).The coordinate of these GCPs were extracted by firstly, navigating the point cloud and find the GCPs in the project since we have already known where GCPs are installed, then add a Tie point at the middle point of GCPs panels, finally we can get actual coordinate of these GCPs and save these Tie points as 3D GCP.

Figure 4. Ground Control Points panel

b) *Flight Planning*

To achieve sufficient and high-quality data images, a good flight planning is the key factor. Thus, the flight altitude, flight path, camera angles, the scale (Ground Sampling Distance or GSD) and overlaps between the different images have been set and calculate with HG Robotic (UAV flight planning) software created by HG Robotic company, Thailand. In this experiment, we use Ground Sampling Distance (GSD) 5 cm which responds to flight height about 73 meters from the ground. As recommend from company for RedEdge camera, at least 75% of frontal and side overlapping should be obtained, so we have set 80% of frontal overlapping and 60% of side overlapping. For camera angle, we chose Nadir image mode.

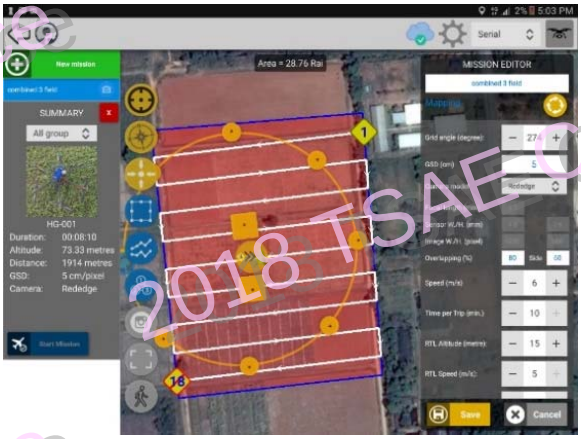

Figure 5. Flight Planning Program

c) Images acquisition

After setting all required options in flight planning program, we tested the compass of the drone by lifting and moving the drone around one round and check whether the signal of drone's direction move to the same direction as the drone's.

As direction from manual of RedEdge camera, we start capturing an image of a calibration reflectance panel (Gray panel) (Figure 6) to create reflectance-compensated outputs. The capture must be completed immediately before and immediately after each flight. The calibrated panel was placed on flat ground and free from illuminated disturbance. Hold the aircraft at chest level and point the camera on the center point of panel and avoid any shadows on panel. Stand in front of the panel and the sun is at your back, and then take a large step to the left or to the right while clicking the Capture button in the camera's WiFi interface page (Tablet). Each mission took time about 9 minutes and capture about 950 images.

Figure 6. Calibrated Gray Panel

2.5 Image Processing

After each flight mission, all images were analyzed in program Pix4D mapper version 4.0 (Pix4D, Switzerland). The first step "Initial processing" will extract keypoints and match those keypoints, and then it corrects internal camera parameters, such as focal length, principal point of autocollimation and lens distortion, and external camera parameters. Afterward, we started to generate the second step "Point Cloud and Mesh" to match pixel, and the third step "DSM, Orthomosaic, and index" to raster Digital Surface Mosaic (DSM), to grid DSM, and orthomosaic. Finally, it produces reflectance map of each band (Blue, Green, Red, NIR, RedEdge). Figure 7. is the flowchart summarizes the process.

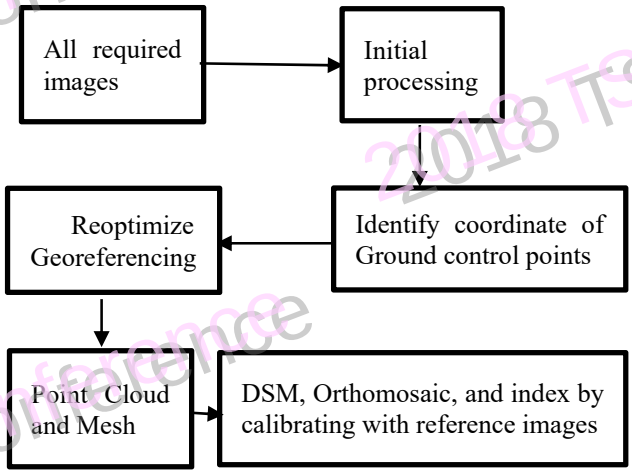

Figure 7. Flowchart of image processing

2.6 Calculation of Vegetation Indices

The 5 band Images of each plot (6x8m, 4 rows) were identified their sizes in pixel and location in reflectance map using boundary of the field as shown in figure 8 which is the reflectance map of blue band captured on 16 November 2017, whose each plot has 155 pixel in width and 115 pixel in height, and then the size of each plot was deducted by 2 pixels from the original size of width and height to remove mixed border pixels and to reduce possibility of errors due to the geometric correction (Lebourgeois et al. (2008)), consequently that plot (figure 8) has size 153 pixel in width and 113 pixel in height that will be used as data for cropping images in Matlab software version 2017. Finally, all reflectance value in that plot was average. This method was applied to all band images in all plots. The size of all images in this study was range from 155 pixels to 165 in width and from 115 pixels to 125 pixels in height.

Figure 8. Reflectance map of blue band, captured on 16 November 2017.

The mean values of each spectral bands in all plot images captured from the four flight dates, were used to derive Vegetation Indices below:

Ration Vegetation Indices (RVI) proposed by (Jordan, 1969) and it was found that can provide estimates of green biomass changes during season (Hatfield et al. (2010)).

$$RVI = \frac{NIR}{R}$$

The Normalized Different Vegetation Indices (NDVI) is used widely as a predictor of Leaf Area Index (LAI) in canopies and more studies have shown that it can accurately estimate seasonal cumulative value of intercepted photosynthetically active radiation (Hatfield et al. (2010)). It is calculated as below:

$$NDVI = \frac{(NIR-R)}{(NIR+R)}$$

The Simple Ration Pigment Index (SRPI) is calculated by dividing the digital value of blue band with the digital value of red band, designed to forecast nitrogen status (Peñuelas et al. (1994)). It has formula as below:

$$SRPIb = \frac{B}{R}$$

Chlorophyll indices green (CI_{green}) and Chlorophyll indices red edge ($CI_{red\ edge}$) were proposed by (Gitelson et al. (2003)) & (Gitelson et al. (2005)) for assessment of chlorophyll content in crop canopies. More studies have confirmed that it is a reliable vegetation indice to estimate leaf chlorophyll because it is sensitive to changes of chlorophyll in leaf during early vegetation stage. They are calculated as below:

$$CIgreen = \frac{NIR}{G} - 1$$

$$CIred\ edge = \frac{NIR}{Red\ edge} - 1$$

Green Normalized Different Vegetation Indices was proposed by (Gitelson et al. (1996)) since its link to chlorophyll concentration. It is calculated as following

$$GNDVI = \frac{NIR-G}{NIR+G}$$

Where B (blue), G (green), R (red) NIR (near infrared) and red-edge are digital values achieved in the blue, green, red, NIR, and red-edge band of multispectral camera after correcting all distortions.

2.7 *Ground Data Measurement*

At the same day of flight mission, Brix data were collected in the field from 10 varieties. ATAGO™ Digital Palette Refractometer, PR-101α (ATAGO CO.,LTD, Japan) (Table 4, Figure 9) was used to measure fresh juice from two stalks of sugarcane in each plot. Before measurement, refractometer was calibrated by using distilled water and the calibrated value is 0.0% Brix, and then the fresh juice was taken out from the middle point of stalk and put on the sensor, we click on Measure button, and get result. Detail of ground sapmples are shown in table 4.

Table 4. Statistical information of reference sapmles

Number of samples	18
Range of brix (^{0}brix)	17.37-21.48
Average (^{0}brix)	19.02
SD (^{0}brix)	1.2
Calibration set	18
Validation set	18

Figure 9. ATAGO™ Digital Palette Refractometer, PR-101α

2.8 Calibration model and validation

Calibration model was established by using simple linear regression models between each of the six vegetation indices and Brix value from the four varieties. R^2 and root mean square error (RMSE) of each prediction model were calculated.

3 Results and Discussion

3.1 Seasonal trends in the crop state variables

Figure 10. shows about the accumulation of brix value in 4 varieties. From overall view, brix content of all variety was increased gradually, but there was a decline in variety UT84-12 and K88-92 during the second week of flight, and in variety KK3 during third flight because land level is not well balance, so some parts of plots are in lower level where encountering irrigated water from nearby fields is not avoidable, that reason can cause brix value decreases. From graph below, variety KK3 and KK06-501 had similarly trend of brix development, and variety UT84-12 and variety K88-92 shared alike brix value pattern too.

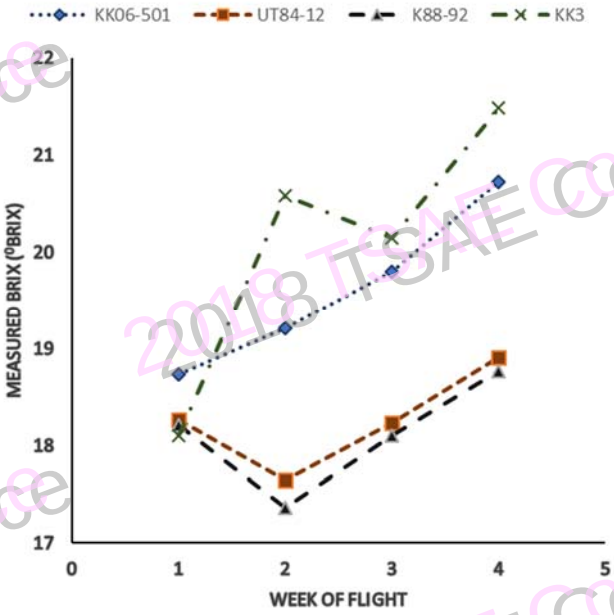

Figure 10 Temporal trends in crop state variables. Time is expressed as week of flight, week 1 (02 Nov 2017), week 2 (09 Nov 2017), week 3 (16 Nov 2017), and week 4 (27 Nov 2017).

3.2 Seasonal trends of the vegetation indices

Figure 11 shows the GNDVI map of the 4-rows sugarcane stalks in KK06-501 variety plot photographed on 16 November 2017. There are 6 noticable colors in GNDVI map that represent in varied range of GNDVI value which can be translated as follwing. The area with red color (0.29-0.50) are bare soil, however there are some parts in the field which actually contained of well-grown sugarcane stalks but were highlighted by red color too, it is because of those specific zone have lodged stalks, so the reflectance that detected by sensor is the rebounced radiation after hitting sugarcane's skin that has dark gray color similar to bare soil. Hence, futher study about distinguishing soil and lodged stalks is required in order to enhacne the calibration model. The orange part (0.50-0.55)represents brix value from 21.48 to 20.15 ^{0}brix and shows a trend of the higher brix value, the lower GNDVI value. The yellowish organge (0.55-0.59) part has brix value 18.73-19.80 ^{0}brix, and the yellow color (0.59-0.65) is equalvalent to brix value 17.37-18.23 ^{0}brix, and last zone is green color (0.65-0.86) which represents lush green leaves.

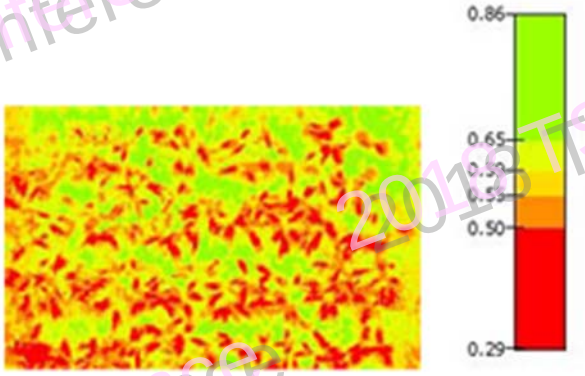

Figure 11. GNDVI map of variety KK06-501 captured on 16 November 2017

All average vegetation indices were plotted with theirs flight dates. GNDVI, CIgreen and CIrededge have almost identical trend which variety KK3 and KK06-501 are stick together, and so do variety UT84-12 and variety K88-92. While other three vegetation indices, NDVI, RVI and SRPIb, the two pairs didn't stay close despite of having comparable shift. From figure 12. It is noticeable that all varieties had vegetation indices values decreased from week to week despite of having brix value increased. It is respond to aging phase of sugarcane when sugar was being produced.

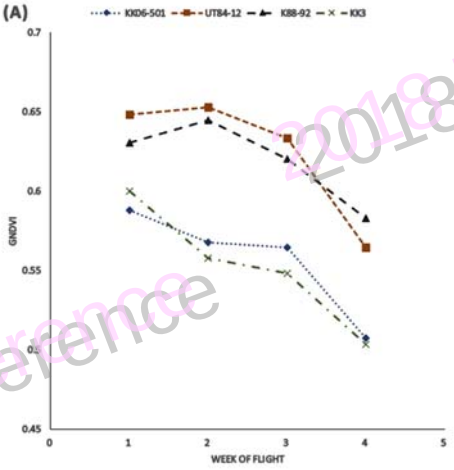

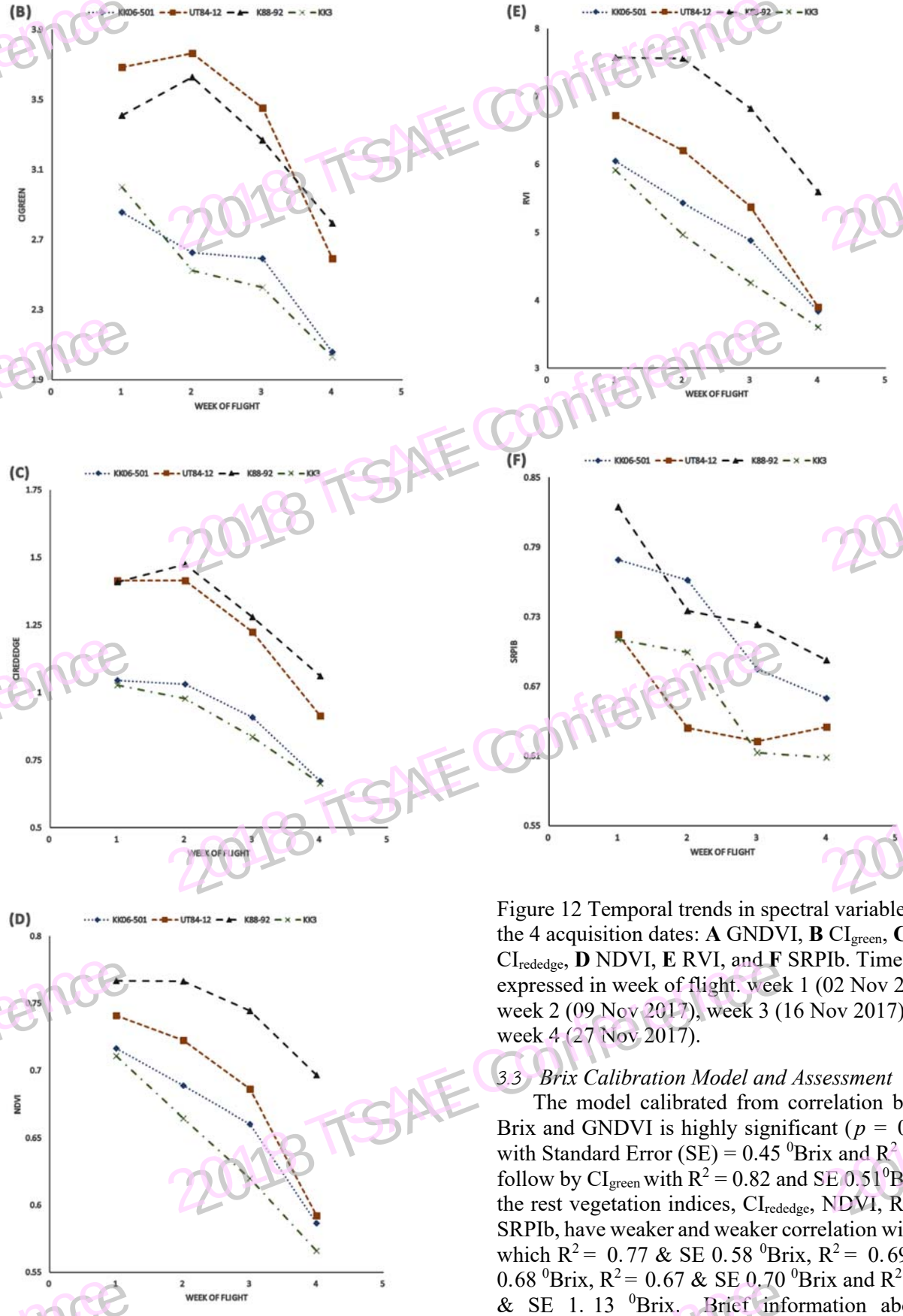

Figure 12 Temporal trends in spectral variables for the 4 acquisition dates: **A** GNDVI, **B** CI_{green}, **C** $CI_{rededge}$, **D** NDVI, **E** RVI, and **F** SRPIb. Time is expressed in week of flight. week 1 (02 Nov 2017), week 2 (09 Nov 2017), week 3 (16 Nov 2017), and week 4 (27 Nov 2017).

3.3 Brix Calibration Model and Assessment

The model calibrated from correlation between Brix and GNDVI is highly significant ($p = 0.005$), with Standard Error (SE) = 0.45 ^{0}Brix and $R^2 = 0.86$, follow by CI_{green} with $R^2 = 0.82$ and SE 0.51 ^{0}Brix and the rest vegetation indices, $CI_{rededge}$, NDVI, RVI and SRPIb, have weaker and weaker correlation with brix, which $R^2 = 0.77$ & SE 0.58 ^{0}Brix, $R^2 = 0.69$ & SE 0.68 ^{0}Brix, $R^2 = 0.67$ & SE 0.70 ^{0}Brix and $R^2 = 0.16$ & SE 1.13 ^{0}Brix. Brief information about all regression models is shown in table 5.

The model calibrated from GNDVI, which is derived from green and NIR band, is the best prediction model. It is explainable by the research of

Junker et al. (2016) found that green and red band are better to detect leaf pigment composition and quantity which have changed continuously during senescence stage and our experiment also conducted in early harvest season when sugarcane was in progress of leaf senescence and brix accumulation. This study result is agreeable with reason above because the model with CI_{green} which is computed from green and NIR band but with different formula has high R^2 nearly equal to GNDVI's. Even though, NDVI is composed with red band, but it has weaker ability to assess canopy 'greenness' since this vegetation indices were influenced by high anthocyanin level in leaves (Junker et al. (2016)).

Figure 13A, B, C, D and E shows that variety UT84-12 and KK3 have a big error of prediction while variety KK06-501 and K88-92 are stayed close to trendline with small error of prediction. Brix value of KK3 and KK06-501 are high, whereas the other two varieties have low brix, so the range of brix doesn't affect on model accuracy, but cultivar does. The result is similar with (Lebourgeois et al. (2012)) found that relation between nitrogen leaf (N_L) with GNDVI and NDVI were slightly influenced by cultivar ($p = 0.005$).

Figure 14. show that KK06-501 has the best prediction, RMSE smaller than 0.1 ^{0}Brix, in almost regressions except linear using SRPIb whose R^2 is the lowest. The second-best prediction is variety K88-92 which has RMSE in range from 0.07-0.59 ^{0}Brix. Then the third and last are UT 84-12 and KK3 respectively.

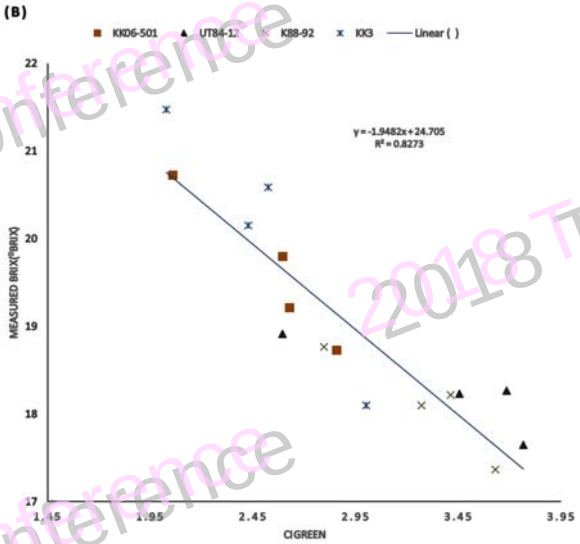

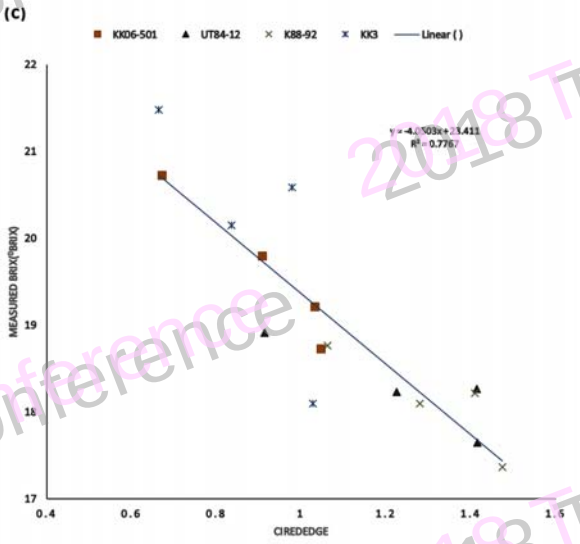

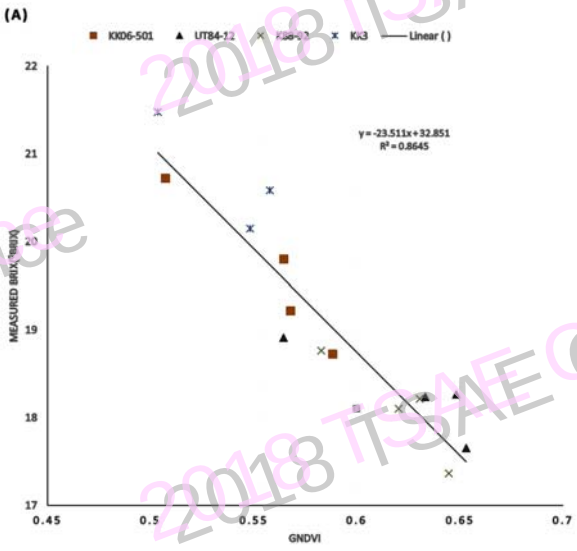

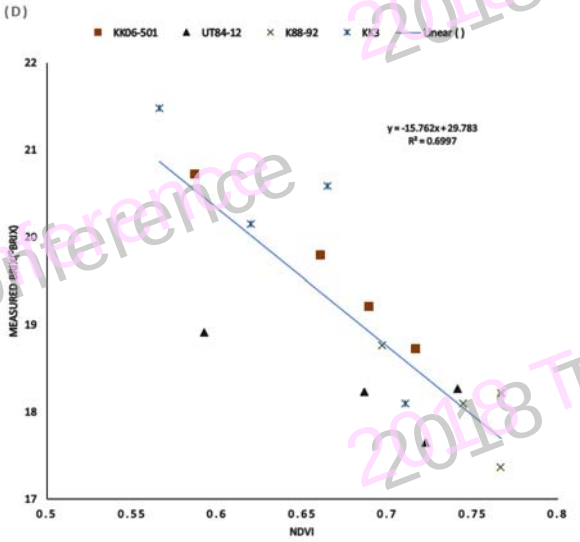

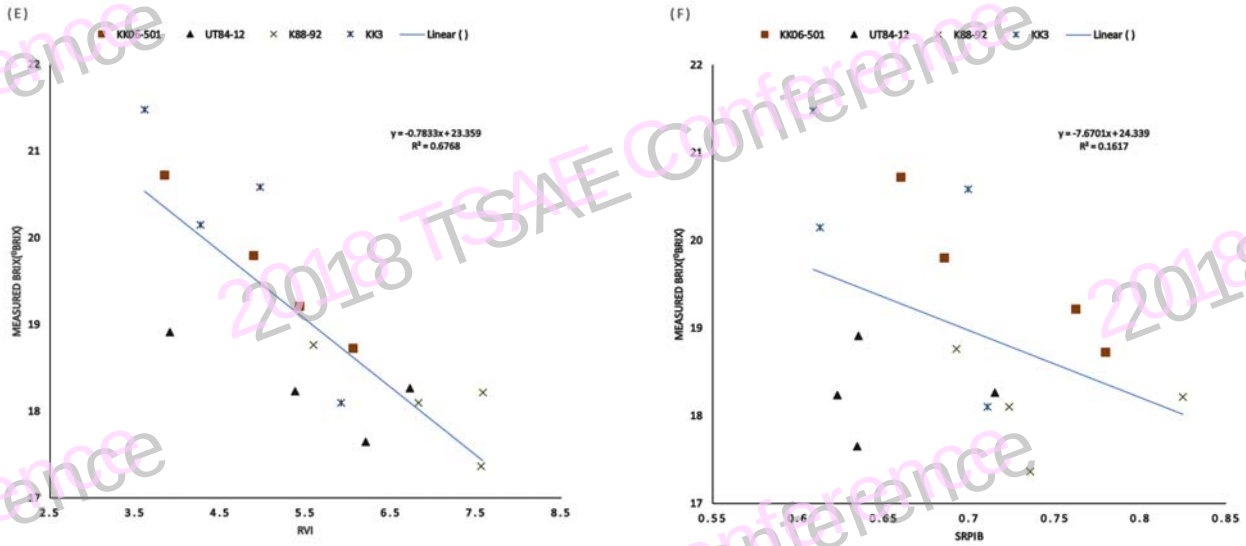

Figure 13. Simple linear regression between Brix and GNDVI **(A)**, CI_{green} **(B)**, NDVI **(C)**, RVI **(D)**, $CI_{rededge}$ **(E)**, and SRPIb **(F).**

Table 5. Coefficient, Model, R^2 and standard error of regression between all VIs and Brix value

VIs	Coefficient	Model	R^2	SE (^{0}Brix)
GNDVI	-23.511	32.851 – 23.511(GNDVI)	0.86	0.45
CI_{green}	-1.9482	24.705 – 1.9482(CI_{green})	0.82	0.51
$CI_{rededge}$	-4.0503	23.411 – 4.0503($CI_{rededge}$)	0.77	0.58
NDVI	-15.762	29.783 – 15.762(NDVI)	0.69	0.68
RVI	-0.7833	23.359 – 0.7833(RVI)	0.67	0.70
SRPIb	-7.6701	24.339 – 7.6701(SRPIb)	0.16	1.13

Table 6. Root Mean Square Error (RMSE) of variety in each model and total RMSE of all regression

Variety	GNDVI	CI_{green}	$CI_{rededge}$	NDVI	RVI	SRPIb
KK06-501	0.06	0.08	0.05	0.08	0.05	0.81
UT84-12	0.24	0.3	0.25	0.87	0.88	1.43
K88-92	0.07	0.1	0.1	0.09	0.17	0.59
KK3	0.34	0.43	0.79	0.56	0.63	1.68
Total RMSE	0.18	0.23	0.3	0.4	0.43	1.13

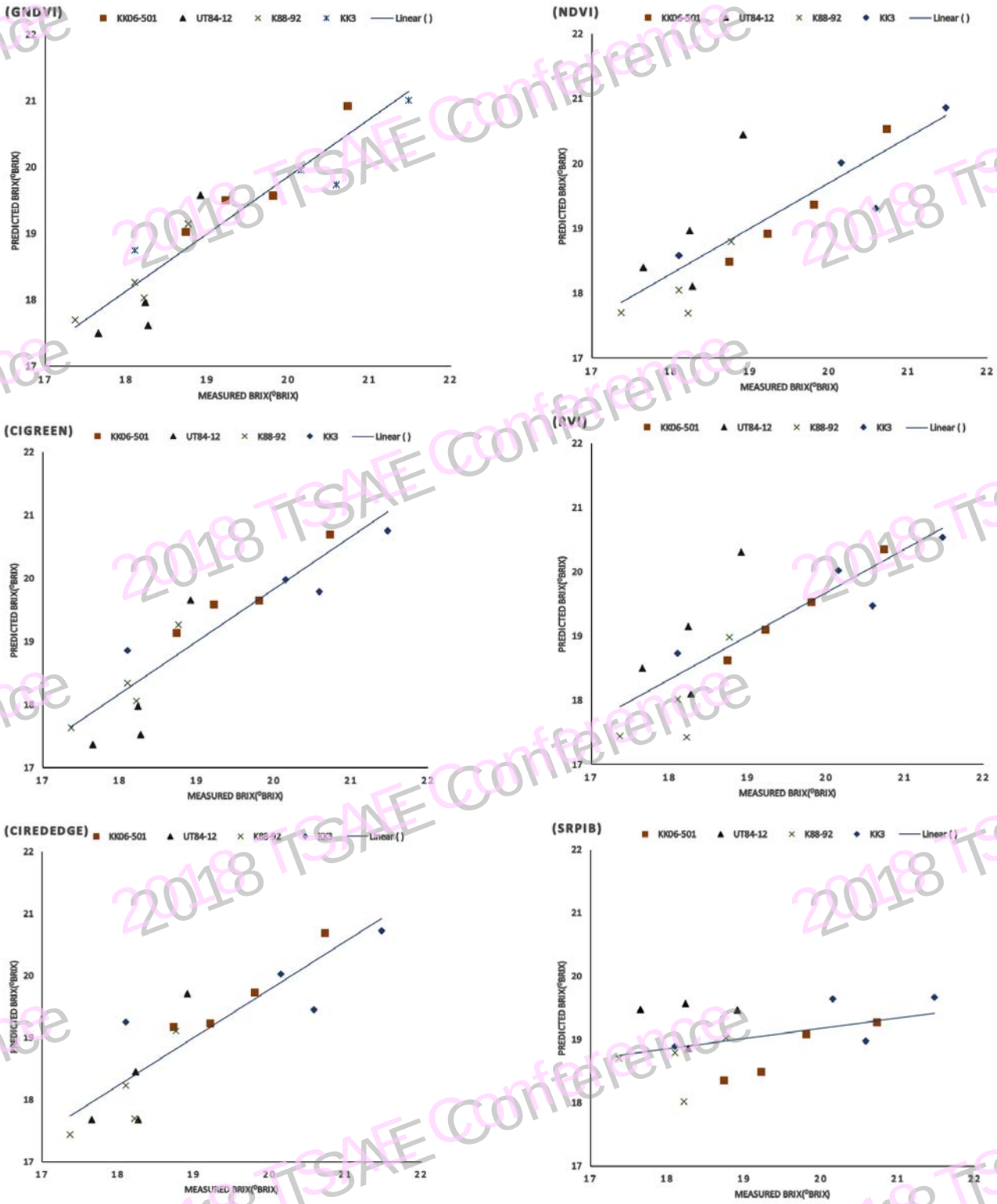

Figure 14. Scatter plot graph between measured brix and predicted brix of regression using GNDVI, CI_{green}, $CI_{rededge}$, NDVI, RVI, and SRPIb.

4 Conclusions

In this study, we investigate possibility of the use of spectra from multispectral camera mounted on UAV to evaluate brix value in sugarcane field. Results show that GNDVI and CI_{green}, calculated from Green and NIR band, were correlated well with brix value. So further researches with more vegetation indices acquired from green band possibly improve the model. However, the relationship of these two vegetation indices with brix value relies on cultivar, but we need further study with more data and statistical method to confirm this outcome. This experiment has some limitations. First, data collection time is in early season when the brix rang is still low. Second, number of reference stalks in study are not sufficient to calibrate an applicable model. Despite these limitations, data of this test is adequate to confirm about potential of building an appropriate prediction model.

5 Acknowledgements

This work has been supported financially by Applied Engineering for Importance Crops of the North East Research Group, Khon Kaen University. The authors are grateful to HG Robotic company, Thailand, for sponsoring Drone and multispectral camera, Northeast Thailand Cane and Sugar Research Center for providing experimental field, and Khon Kean Field Crop Research Center for supplying chemical substance and equipment to this experimental study. The authors thank Kanvisit Maraphum, Arthit Phuphaphud, Khanittha Thaveesaeng for their assistance with data collection.

6 References

3D Robotics, Inc. . Pixhawk. Available online: https://store.3dr.com/t/pixhawk (accessed on 07 December 2017)

ATAGO CO., LTD, ATAGO™ Digital Palette Refractometer, PR- 101α. Available online: http://www.atago.net/product/?l=en&f=products_pr.php (accessed on 02 December 2017)

Baluja J, Diago MP, Balda P, Zorer R, Meggio F, Morales F, et al. 2012. Assessment of vineyard water status variability by thermal and multispectral imagery using an unmanned aerial vehicle (UAV). Journal of Irrigation Science 30(6), 511–22.

Berni J, Zarco- Tejada PJ, Suarez L, Fereres E. 2009. Thermal and Narrowband Multispectral Remote Sensing for Vegetation Monitoring From an Unmanned Aerial Vehicle. Journal of IEEE Transactions on Geoscience and Remote Sensing 47(3) , 722– 38. Available from: http://ieeexplore.ieee.org/document/4781575/

Flynn KF, Chapra SC. 2014. Remote sensing of submerged aquatic vegetation in a shallow non-turbid river using an unmanned aerial vehicle. Journal of Remote Sensing 6(12), 12815–36.

Gitelson, A. A., Kaufman, Y. J., & Merzlyak, M. N. 1996. Use of a green channel in remote sensing of global vegetation from EOS-MODIS. Journal of Remote Sensing of Environment 58, 289–298.

Gitelson, A.A., Vina, A., Ciganda, V., Rundquist, D. C. and Arkebauer, T. J. , 2005. Remote estimation of canopy chlorophyll content in crops. Journal of Geophysical Research Letters 32.

Gitelson, A. A.; Gritz, U.; Merzlyak, M.N. 2003. Relationships between leaf chlorophyll content and spectral reflectance and algorithms for non-destructive chlorophyll assessment in higher plant leaves. Journal of Plant Physiology 160, 271-282.

Hatfield JL, Prueger JH. 2010. Value of using different vegetative indices to quantify agricultural crop characteristics at different growth stages under varying management practices. Journal of Remote Sensing 2(2), 562–78.

Jordan, C.F. 1969. Derivation of leaf area index from quality of light on the forest floor. Journal of Ecology 50, 663- 666.

Junker LV, Ensminger I. 2016. Relationship between leaf optical properties, chlorophyll fluorescence and pigment changes in senescing Acer saccharum leaves. Journal of Tree Physiology 36, 694-711.

Laliberte AS, Goforth MA, Steele CM, Rango A. 2011. Multispectral remote sensing from unmanned aircraft: Image processing workflows and applications for rangeland environments. Journal of Remote Sensing 3(11), 2529–51.

Lebourgeois V, Bégué A, Labbé S, Houlès M, Martiné JF. 2012. A light-weight multi-spectral aerial imaging system for nitrogen crop monitoring. Journal of Precision Agriculture 13, 525–41.

Lebourgeois V, Bégué A, Labbé S., Mallavan, B., Prévot, L., & Roux, B. 2008. Can commercial digital cameras be used as multispectral sensors? A crop monitoring test. Journal of Sensors 8, 7300–7322.

Mat Nawi N, Chen G, Jensen T, Mehdizadeh SA. 2013. Prediction and classification of sugar content of sugarcane based on skin scanning using visible and shortwave near infrared. Journal of Biosystems Engineering 115(2) , 154– 61. Available from: http://dx.doi.org/10.1016/j.biosystemseng.2013.03.005

Mat NN, Rowshon KM, Guangnan C, Troy J. 2014. Prediction of Sugarcane Quality Parameters Using Visible- shortwave Near Infrared Spectroradiometer. Journal of Agriculture and Agricultural Science Procedia 2, 136– 43. Available from: http://linkinghub.elsevier.com/retrieve/pii/S2210784314000217

MicaSense. RedEdge camera. Available online: https: / / www. micasense. com/ rededge/ (accessed on 01 December 2017)

MSF Sugar PTY LTD (AU). 2016. Cane Pricing Guide. Available at: https: / / www. msfsugar. com. au/ wp-content/ uploads/ 2016/ 08/ MSF- Sugar- Cane-Pricing- Guide- 2016. pdf. Accessed on 12 December 2017

Peñuelas, J., Gamon, J.A., Fredeen, A.L., Merino, J. and Field, C.B., 1994. Reflectance indices associated with physiological changes in nitrogen- and water- limited sunflower leaves. Remote sensing of Environment 48,135-146.

Pix4D. Pix4Dmapper, Photogrammetry software for professional drone- based mapping purely from images. Versions 4.0. Available online: https: / / pix4d. com/ product/ pix4dmapper-photogrammetry- software/ (accessed on 01 December 2017)

Wojtowicz M, Wojtowics A, Piekarczyk J. 2015. Application of remote sensing methods in Agriculture. Journal of Communications in Biometry and Crop Science 11, 31–50.